



35 The ionosphere is the part of the atmosphere at the altitudes of 60 km to 1,100 km where there
36 are ions and free electrons in considerable amounts that can reflect electromagnetic waves. It
37 completely covers the thermosphere, one of the main layers of the atmosphere, but also includes
38 some of the mesosphere and the exosphere.

39 The most important parameter that defines the ionosphere in space and time is the quantity of
40 electrons. This quantity varies under the influence of the day-night cycle, seasons, geographical
41 location and magnetic storms in the sun. As it is not possible to measure the quantity of electrons
42 in the ionosphere directly, indirect measurement and calculation methods have been developed
43 (Li and Parrot, 2018). Total Electron Content (TEC), which is defined as the quantity of free
44 electrons along a cylinder with a cross section of 1 m^2 , is a suitable parameter to monitor the
45 changes in the ionosphere in space and time. All signals that contain audio and data that pass
46 through or get reflected from the ionosphere, which is highly irregular and difficult to model,
47 are affected by the structure of this layer.

48 Calculating Total Electron Content (TEC) is a method used directly to investigate the structure
49 of the ionosphere. TEC is represented by the unit of TECU, and one TECU equals to
50 10^{16} el/m^2 (Schaer, 1999). TEC is expressed in two ways: STEC (Slant Total Electron
51 Content); the free electron content calculated along the slanted line between the receiver and
52 the satellite, and VTEC (Vertical Total Electron Content); the free electron content calculated
53 along the zenith of the receiver (Langley, 2002).

54 TEC varies based on positional and temporal variables such as the latitude of the place, seasons,
55 solar activity, geomagnetic storms and earthquakes. Ionospheric altitude also differs based on
56 geography.

57 TEC, which is defined as the number of free electrons on the one square meter area on the line
58 followed by a radio wave, is one of the important parameters for examining the structure of the
59 ionosphere and the upper atmosphere. With TEC values, it is possible to examine the short and
60 long-term changes in the ionosphere, ionospheric irregularities and disruptive factors together
61 (Erol and Arıkan 2005).

62 Ionospheric changes are being studied in more than twenty countries today as precursors of
63 earthquakes. Definition of ionospheric anomalies and feasibility studies of seismo-ionospheric
64 precursors are still ongoing (Akhoondzadeh et al., 2018; Liu et al., 2010; He et al., 2012;
65 Kamogawa and Kakinami, 2013; Heki and Enomoto, 2015; Pulnits and Davidenko, 2014;
66 Masci et al., 2015; Yildirim et al., 2016; He and Heki, 2017; Kelley et al., 2017; Rozhnoi et al.,
67 2015; Thomas et al., 2017).



68 **2. METHODOLOGY**

69 **2.1 IONOLAB-TEC Method:**

70 The IONOLAB-TEC method developed by the department of Electrical and Electronics
71 Engineering of Hacettepe University is a JAVA application that uses the Regularized TEC (D-
72 TEI) algorithm (Arikan et al. 2004).

73 In this application, they developed a method that estimates VTEC values by using all GPS
74 signals measured at a period of time in a day. While the measurements taken from the satellites
75 with elevations of 60° or higher are used, the measurements from the satellites with elevations
76 of 10° to 60° are weighted by a Gauss function. The data from satellites with elevations of
77 lower than 10° are not included in calculations to reduce multipath effects. In this method raw
78 GPS data was used to determine VTEC value.

79

80 **2.2 Global Ionosphere Model (GIM):**

81

82 Global Ionospheric Maps are published in the IONEX (IONosphere map EXchange) format in
83 a way that covers the entire world. The institutions that produce these maps in the world include
84 CODE (Center for Orbit Determination in Europe, Switzerland), DLR (Fernerkundungstation
85 Neustrelitz, Germany), ESOC (European Space Operations Centre, Germany), JPL (Jet
86 Propulsion Laboratory, California), NOAA (National Oceanic and Atmospheric
87 Administration, United States), NRCan (National Resources, Canada), ROB (Royal
88 Observatory of Belgium, Belgium), UNB (University of New Brunswick, Canada), UPC
89 (Polytechnic University of Catalonia, Spain), WUT (Warsaw University of Technology,
90 Poland). In this study we used the GIM-TEC values produced by CODE in the IONEX format.
91 In the dates they were analyzed, the temporal resolution of the TEC values was 2 hours, while
92 their positional resolution was 2.5° by latitude and 5° by longitude. In order to calculate TEC
93 values for a point whose latitude and longitude is known on the GIM-TEC maps created by
94 CODE using more than 300 GNSS receivers around the world, the 4 TEC values that cover the
95 point and the two-variable interpolation formula are given below.

96 $E_{int}(\lambda_0 + p\Delta\lambda, \beta_0 + q\Delta\beta) = (1 - p)(1 - q)E_{0,0} + p(1 - q)E_{1,0} + q(1 - p)E_{0,1} + pqE_{1,1} \quad (1)$

97 p and q : $0 \leq p, q < 1$.

98 $\Delta\lambda$ and $\Delta\beta$: Longitude and Latitude differences grid widths,

99 λ_0 and β_0 : Initial longitude and latitude values,

100 $E_{0,0}, E_{1,0}, E_{0,1}$ ve $E_{1,1}$: TEC values known in neighboring points,

101 E_{int} : TEC value to be found.

102



103 **3. ANALYSIS TO DETERMINE EARTHQUAKE-RELATED TEC CHANGES**

104
 105 In order to investigate earthquake-related TEC changes, the TEC values for the stations close
 106 to the epicenters, HAKK, MALZ, OZAL and TVAN (TUSAGA-Aktive CORS-TR) GPS
 107 stations were analyzed to determine TEC value using the IONOLAB-TEC and GIM-TEC
 108 models. The correlation coefficient was obtained for the TEC values from both models between
 109 the dates 13.10.2011 and 02.11.2011 for the stations above.



110
 111 **Figure 1.** Analyzed Stations

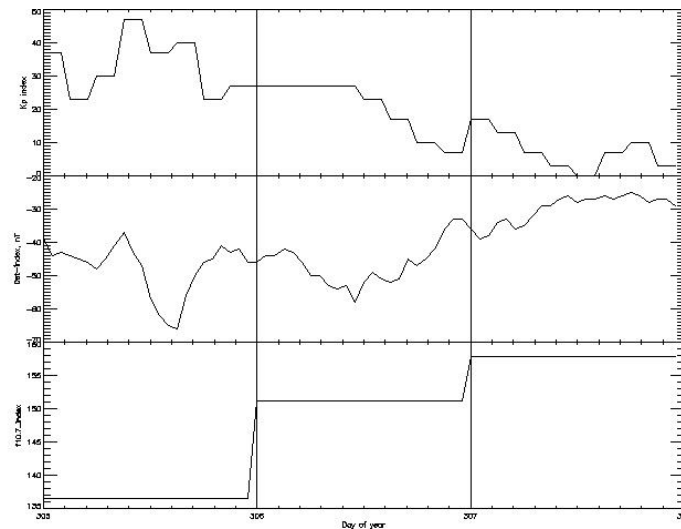
112 Figure 1 shows the stations analyzed (represented by red triangles) and the epicenter of the
 113 earthquake represented by blue star. For each station, the TEC values with the temporal
 114 resolution of two hours obtained from both the IONOLAB-TEC and GIM-TEC models and the
 115 correlation coefficient showing whether there is a linear relationship between two values were
 116 calculated as below;

117
 118
$$r = \frac{\Sigma(xy) - (\Sigma x)(\Sigma y)/n}{\sqrt{(\Sigma x^2 - (\Sigma x)^2/n)(\Sigma y^2 - (\Sigma y)^2/n)}} \quad (2)$$

119
 120 In order to determine the outlier values among the TEC values with a two-hour temporal
 121 resolution from both models, the TEC values obtained from both models between the dates
 122 01.10.2011 and 10.10.2011, which were considered quiet in terms of geomagnetic and solar
 123 activity, were used to determine the upper boundary (UB) and the lower boundary (LB). By

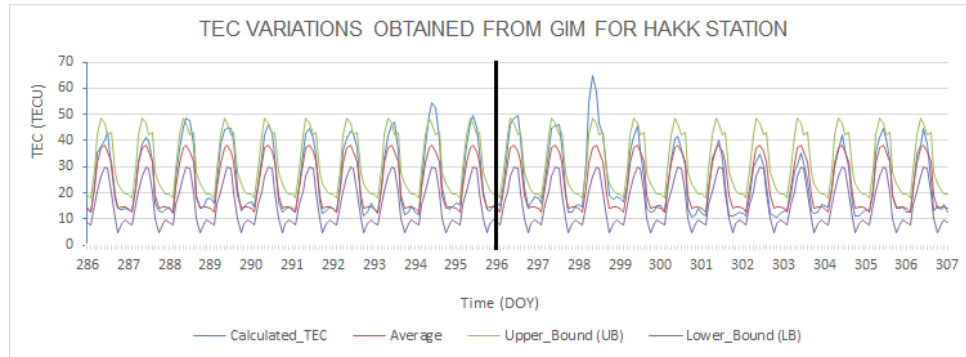


124 utilizing the TEC values from both models, the UB and LB values were calculated using the
125 formulae $x+3\sigma$ and $x-3\sigma$. Here, x is the mean TEC value for the relevant epoch and σ is the
126 standard deviation. If the TEC value in any epoch is higher than the upper boundary, it is a
127 positive anomaly. Similarly if it is lower than the lower boundary, it is a negative anomaly. In
128 order to investigate whether the anomalies before, on the day of and after the earthquake were
129 caused by the earthquake or not, we also examined the (Kp*10), Dst and F10.7 cm indices,
130 which provided information on the geomagnetic and solar activity for the days in which
131 anomalies were detected.
132



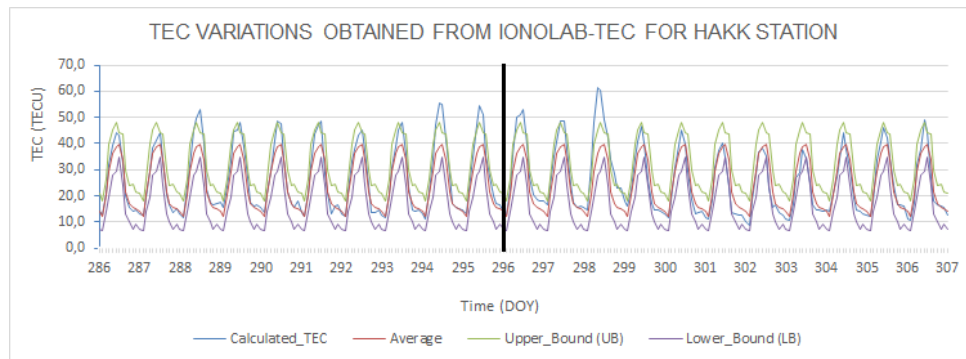
133
134 **Figure 2.** The Chart for the Dates 01-03.11.2011 in (Kp*10), Dst and F10.7 cm Indices
135 (URL-1)
136

137 Figures 2 shows that the (Kp*10), Dst and F10.7 cm indices that provide information on
138 geomagnetic and solar activity in October and on the first three days of November. Below are
139 the TEC values for the HAKK station for the dates 13.10.2011-02.11.2011 obtained using the
140 GIM-TEC and IONOLAB-TEC methods.
141



142
 143
 144

Figure 3. GIM-TEC Values for the HAKK Station



145
 146
 147

Figure 4. IONOLAB-TEC Values for the HAKK Station

148 The correlation coefficient r between the TEC values calculated by both methods for the HAKK
 149 station was 0.98 indicating a strong positive relationship. The anomaly tables for this station
 150 are provided below (Tables 1 and 2).

151

GIM-TEC Anomaly Table for HAKK Station									
Number	DOY	Hour	TEC Difference (TECU)	Type of Anomaly	Number	DOY	Hour	TEC Difference (TECU)	Type of Anomaly
1	286	12	1.0	Positive	7	294	12	10.5	Positive
2	288	12	5.7	Positive	8	295	12	7.3	Positive
3	289	12	2.5	Positive	9	296	12	7.5	Positive
4	290	12	0.5	Positive	10	297	12	4.1	Positive
5	292	12	0.8	Positive	11	298	8	16.5	Positive
6	293	12	5.2	Positive					

152

Table 1. HAKK Station Global Ionosphere Model Anomaly Table



153

IONOLAB-TEC Anomaly Table for HAKK Station									
Number	DOY	Hour	TEC Difference (TECU)	Type of Anomaly	Number	DOY	Hour	TEC Difference (TECU)	Type of Anomaly
1	287	12	0.4	Positive	9	295	12	7.2	Positive
2	288	12	9.2	Positive	10	296	12	8.8	Positive
3	289	12	4.3	Positive	11	297	12	4.6	Positive
4	290	12	3.8	Positive	12	298	8	16.5	Positive
5	291	12	4.5	Positive	13	301	12	0.3	Negative
6	292	12	1.4	Positive	14	302	14	0.9	Negative
7	293	12	4.2	Positive	15	303	12	0.7	Negative
8	294	12	10.9	Positive	16	306	10	0.9	Positive

154

Table 2. HAKK Station IONOLAB-TEC Anomaly Table

155

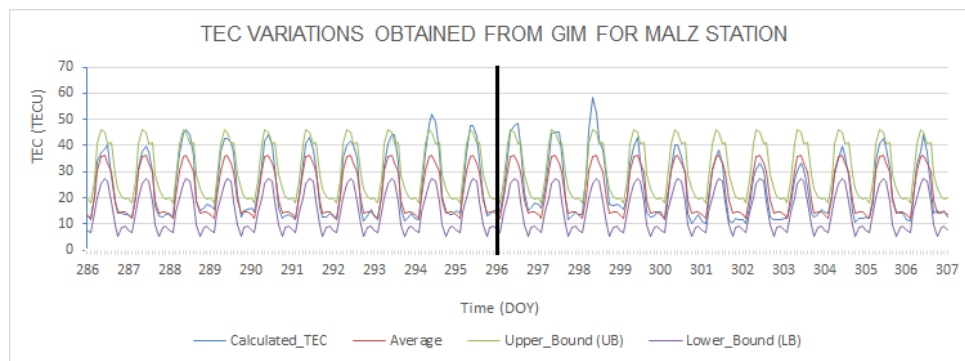
156

Below are the TEC values for the MALZ station obtained using the GIM-TEC and IONOLAB-

157

TEC methods (Figures 5 and 6).

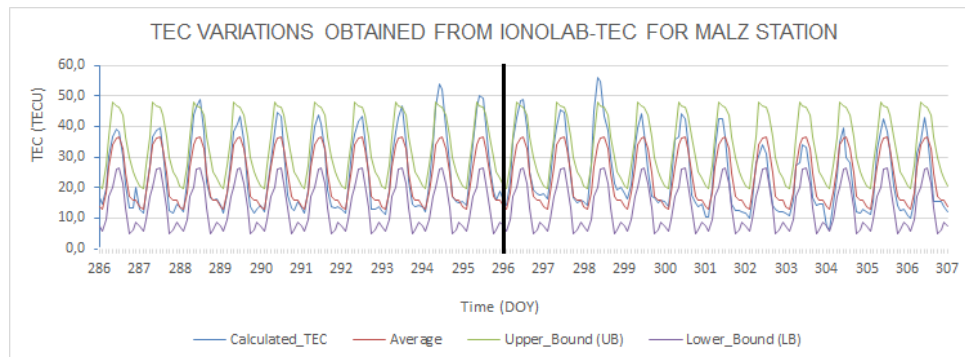
158



159

160

Figure 5. GIM-TEC Values for the MALZ Station



161

162

Figure 6. IONOLAB-TEC Values for the MALZ Station



163

164 The correlation coefficient r between the TEC values calculated by both methods for the MALZ
 165 station was 0.98 indicating also a strong positive relationship. The anomaly tables for this
 166 station are provided below (Tables 3 and 4).

167

GIM-TEC Anomaly Table for MALZ Station									
Number	DOY	Hour	TEC Difference (TECU)	Type of Anomaly	Number	DOY	Hour	TEC Difference (TECU)	Type of Anomaly
1	288	12	3.5	Positive	5	295	12	3.1	Positive
2	289	12	0.5	Positive	6	296	12	7.9	Positive
3	293	12	3.9	Positive	7	297	12	4.7	Positive
4	294	12	8.6	Positive	8	298	8	12.6	Positive

168

Table 3. MALZ Station Global Ionosphere Model Anomaly Table

169

170

IONOLAB-TEC Anomaly Table for MALZ Station									
Number	DOY	Hour	TEC Difference (TECU)	Type of Anomaly	Number	DOY	Hour	TEC Difference (TECU)	Type of Anomaly
1	288	12	2.3	Positive	5	296	12	2.5	Positive
2	293	12	0.4	Positive	6	298	6	8.6	Positive
3	294	10	7.4	Positive	7	304	0	0.2	Negative
4	295	10	3.6	Positive					

171

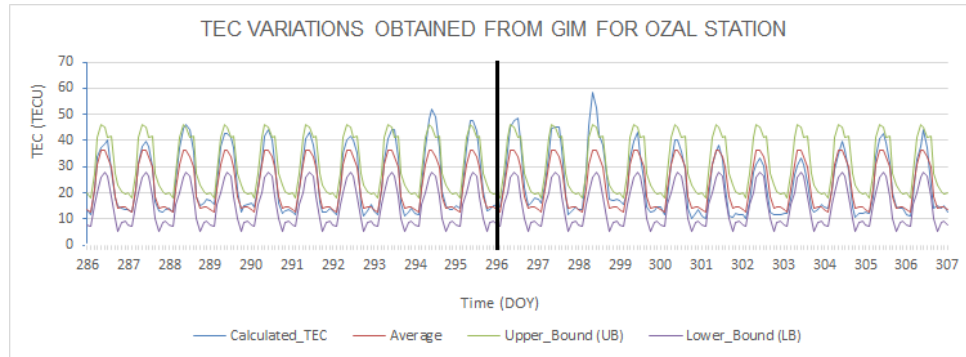
Table 4. MALZ Station IONOLAB-TEC Anomaly Table

172 Tables 3 and 4 show the anomalies found as a result of the analysis of the TEC values obtained
 173 by the IONOLAB-TEC and GIM-TEC methods for the MALZ station. It is believed that the
 174 positive anomaly on days 288 and 289 was caused by moderate (136.9 sfu, 150 sfu) solar
 175 activity. It is also believed that the anomalies on the days 293, 294, 295 and 296 were caused
 176 by strong (157.8 sfu, 166.3 sfu, 162.5 sfu, 153.9 sfu) solar activity.

177

178 Below are the TEC values for the OZAL station obtained using the GIM-TEC and IONOLAB-

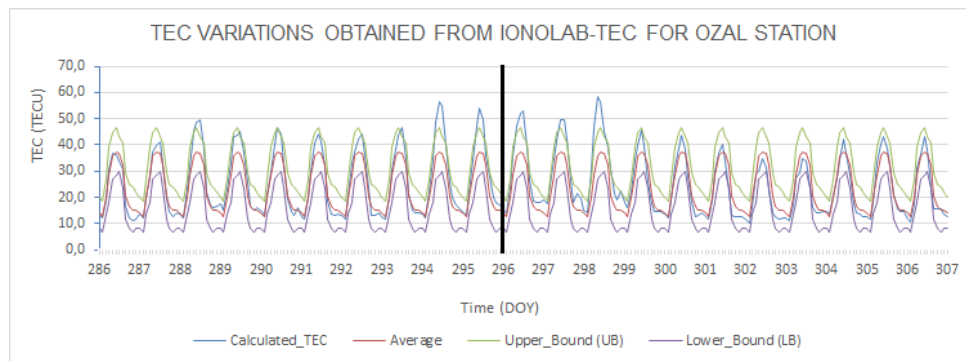
179 TEC methods for the dates 13 October – 02 November (Figures 7 and 8).



180

181

Figure 7. GIM-TEC Values for the OZAL Station



182

183

Figure 8 IONOLAB-TEC Values for the OZAL Station

184

185 The correlation coefficient r between the TEC values calculated by both methods for the OZAL
 186 station was 0.98 demonstrating a strong positive relationship. The anomaly tables for this
 187 station are provided below (Tables 5 and 6).

188

GIM-TEC Anomaly Table for OZAL Station									
Number	DOY	Hour	TEC Difference (TECU)	Type of Anomaly	Number	DOY	Hour	TEC Difference (TECU)	Type of Anomaly
1	288	12	2.8	Positive	5	296	12	7.2	Positive
2	293	12	3.2	Positive	6	297	12	4.0	Positive
3	294	12	7.9	Positive	7	298	8	12.4	Positive
4	295	12	2.4	Positive					

189

Table 5. OZAL Station Global Ionosphere Model Anomaly Table

190

191



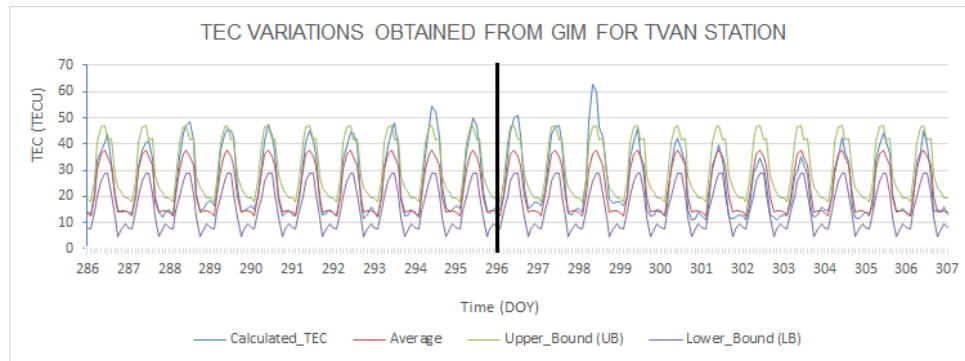
IONOLAB-TEC Anomaly Table for OZAL Station									
Number	DOY	Hour	TEC Difference (TECU)	Type of Anomaly	Number	DOY	Hour	TEC Difference (TECU)	Type of Anomaly
1	288	12	6.1	Positive	7	295	10	7.4	Positive
2	289	12	1.6	Positive	8	296	12	9.6	Positive
3	290	12	0.9	Positive	9	297	12	6.0	Positive
4	293	12	3.5	Positive	10	298	8	13.6	Positive
5	292	12	0.6	Positive	11	301	14	1.2	Negative
6	294	12	11.8	Positive	12	302	14	1.4	Negative

192 **Table 6.** OZAL Station IONOLAB-TEC Anomaly Table

193

194 Below are the TEC values for the TVAN station obtained using the GIM-TEC and IONOLAB-
 195 TEC methods (Figures 9, 10).

196

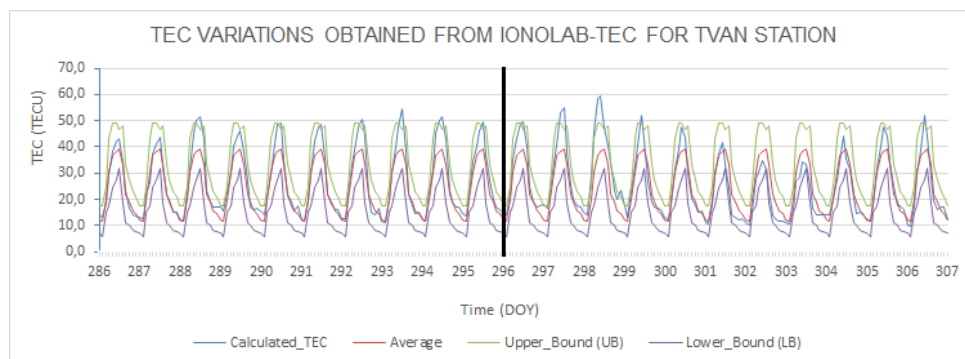


197

198

Figure 9. GIM-TEC Values for the TVAN Station

199



200

201

Figure 10. IONOLAB-TEC Values for the TVAN Station



202 The correlation coefficient between the TEC values calculated by both methods for the TVAN
 203 station was 0.98 representing a strong positive relationship. The anomaly tables for this station
 204 are provided below (Tables 7 and 8).

GIM-TEC Anomaly Table for TVAN Station									
Number	DOY	Hour	TEC Difference (TECU)	Type of Anomaly	Number	DOY	Hour	TEC Difference (TECU)	Type of Anomaly
1	286	12	2.1	Positive	10	294	12	11.0	Positive
2	288	12	7.0	Positive	11	295	12	5.4	Positive
3	289	12	3.5	Positive	12	296	12	9.3	Positive
4	290	12	1.8	Positive	13	297	12	5.5	Positive
5	292	12	2.8	Positive	14	298	8	16.5	Negative
6	293	12	6.4	Positive					

205 **Table 7.** TVAN Station Global Ionosphere Model Anomaly Table

206

IONOLAB-TEC Anomaly Table for TVAN Station									
Number	DOY	Hour	TEC Difference (TECU)	Type of Anomaly	Number	DOY	Hour	TEC Difference (TECU)	Type of Anomaly
1	288	12	5.1	Positive	10	296	12	3.4	Positive
2	290	12	2.6	Positive	11	297	12	8.5	Positive
3	291	12	2.0	Positive	12	298	10	10.5	Positive
4	292	12	4.0	Positive	13	299	10	2.8	Positive
5	293	12	8.1	Positive	14	302	12	0.7	Negative
6	294	12	5.1	Positive	15	306	10	2.9	Positive
7	295	12	3.2	Positive					

207 **Table 8.** TVAN Station IONOLAB-TEC Anomaly Table

208

209 Tables 1, 2, 3, 4, 5, 6, 7 and 8 show the results of the statistical analysis of the TEC values
 210 created by the IONOLAB-TEC and GIM-TEC methods. The tables also depict the day and hour
 211 in which anomalies were observed, and the quantity and type of the anomaly. The numbers of
 212 anomalies obtained in both models were very close to each other. The F10.7 cm index values
 213 between the days 286 and 292 were 136 sfu, 135.4 sfu, 136.9 sfu, 150 sfu, 151.6 sfu, 145.7 sfu,
 214 146.1 sfu. The index values show that there was usually moderate solar activity. Therefore, the
 215 anomalies in question may be related to the earthquake or solar activity. The index values for
 216 the days 293, 294, 295 and 296 (the day of the earthquake) were 157.8 sfu, 166.3 sfu, 162.5 sfu
 217 and 153.9 sfu respectively. These values indicate strong solar activity. On the other hand, the
 218 ionosphere layer was quiet in these days in terms of geomagnetic conditions. As there was
 219 strong solar activity, the numbers of anomalies were higher than the numbers in the days 286-



220 292. Since solar activity was moderate in the day 297, the number of anomalies dropped. The
221 solar activity on the day 298 was moderate, but there was strong geomagnetic activity (Dst -
222 147 nt, $K_p^*10=73$). The reason for the high numbers of anomalies on day 298 in both models
223 is believed to be due to geomagnetic activity. Considering the analyzed days in general, it may
224 be seen that it is difficult to identify earthquake-related anomalies as the solar activity and
225 geomagnetic conditions before and after the earthquake were not quiet. Therefore, it is believed
226 that the anomalies detected in the stations on days 293-296 may be related to the earthquake
227 and/or solar activity, and the anomalies on days 297 and 298 may be related to the earthquake,
228 solar activity and/or geomagnetic activity.

229 4. CONCLUSION

230 In the scope of this study, the TEC values for the stations HAKK, MALZ, OZAL, TVAN were
231 obtained using the GIM-TEC and IONOLAB-TEC methods. In the comparison of the obtained
232 values, it was seen that there was high correlation between the TEC values obtained by the two
233 models. In order to detect earthquake-related TEC changes better, the TEC values created from
234 both models for the period of 13.10.2011-02.11.2011 were used as reference to determine the
235 UB and LB values. As a result of the statistical test, anomalies were found in all analyzed
236 stations for before, on the day of and after the earthquake. In order to understand whether the
237 anomalies obtained in both models were earthquake-related, the ionospheric conditions,
238 geomagnetic activity and solar activity on the analyzed days were examined using the K_p , Dst
239 and F10.7 cm indices.

240 Consequently, it was determined that the positive anomalies observed on days 286-292 may be
241 related to moderate solar activity and/or the earthquake, and the positive anomalies observed
242 on days 293, 294, 295, 296 (day of the earthquake) may be related to strong solar activity and/or
243 the earthquake. Moderate solar activity and strong geomagnetic activity were observed for day
244 298, so the numbers of anomalies in both models increased dramatically. This increase is
245 considered to be related to geomagnetic activity. The anomaly on day 298 may be related to the
246 earthquake, geomagnetic effects and/or solar activity. The finding that the ionospheric
247 conditions were variable in the analyzed days makes it highly difficult to identify earthquake-
248 related ionospheric changes. Therefore, interdisciplinary studies are needed to determine the
249 earthquake-related part of the change in question.

250

251

252

253



254 **REFERENCES**

- 255 Arikan, F., Erol, C. B., Arikan, O.: Regularized Estimation of Vertical Total Electron Content
256 from GPS Data for a Desired Time Period, *Radio Science*, 39:RS6012, 2004.
- 257 Erol, C.B., Arikan, F.: Statistical Characterization of the Ionosphere Using GPS Signals., *J. of*
258 *Electromagnetic Waves and Appl.*, Vol.19, No:3, 2005.
- 259 He, L., and Heki, K.: Ionospheric anomalies immediately before Mw 7.0-8.0
260 earthquakes. *Journal of Geophysical Research: Space Physics*, 2017.
- 261 He, L., Wu, L., Pulinet, S., Liu, S., Yang, F. A.: Nonlinear background removal method for
262 seismo-ionospheric anomaly analysis under a complex solar activity scenario: A case
263 study of the M9.0 Tohoku earthquake. *Advances in Space Research*, 50(2), 211-220,
264 2012.
- 265 Heki, K. and Enomoto, Y.: Mw dependence of the preseismic ionospheric electron
266 enhancements. *Journal of Geophysical Research: Space Physics*, 120(8), 7006-7020,
267 2015.
- 268 Kelley, M. C., Swartz, W. E., Heki, K.: Apparent ionospheric total electron content variations
269 prior to major earthquakes due to electric fields created by tectonic stresses. *Journal*
270 *of Geophysical Research: Space Physics*, 2017.
- 271 Kamogawa, M. and Kakinami, Y.: Is an ionospheric electron enhancement preceding the 2011
272 Tohoku-Oki earthquake a precursor?. *Journal of Geophysical Research: Space*
273 *Physics*, 118(4), 1751-1754, 2013.
- 274 Langley R. B.: Monitoring the Ionosphere and Neutral Atmosphere with GPS Division of
275 Atmospheric and Space Physics Workshop, Fredericton, N.B., 2002.
- 276 Li, M. and Parrot, M.: Statistical analysis of the ionospheric ion density recorded by DEMETER
277 in the epicenter areas of earthquakes as well as in their magnetically conjugate point
278 areas. *Advances in Space Research*, 2017.
- 279 Liu, J. Y., Chen, C. H., Chen, Y. I., Yang, W. H., Oyama, K. I., Kuo, K. W.: A statistical study
280 of ionospheric earthquake precursors monitored by using equatorial ionization
281 anomaly of GPS TEC in Taiwan during 2001–2007. *Journal of Asian Earth*
282 *Sciences*, 39(1-2), 76-80, 2010.
- 283 Masci, F., Thomas, J. N., Villani, F., Secan, J. A., Rivera, N.: On the onset of ionospheric
284 precursors 40 min before strong earthquakes. *Journal of Geophysical Research: Space*
285 *Physics*, 120(2), 1383-1393, 2015.
- 286 Pulinet S. A.: Strong earthquakes prediction possibility with the help of top side sounding from
287 satellites. *Advances in Space Research* 21(3): 455–458, 1998.



- 288 Pulinet, S. and Davidenko, D.: Ionospheric precursors of earthquakes and global electric
289 circuit. *Advances in Space Research*, 53(5), 709-723, 2014.
- 290 Rozhnoi, A., Solovieva, M., Parrot, M., Hayakawa, M., Biagi, P. F., Schwingenschuh, K.,
291 Fedun, V.: VLF/LF signal studies of the ionospheric response to strong seismic activity
292 in the Far Eastern region combining the DEMETER and ground-based
293 observations. *Physics and Chemistry of the Earth, Parts A/B/C*, 85, 141-149, 2015.
- 294 Schaer S.: Mapping and Predicting the Earth's Ionosphere Using the Global Positioning System,
295 Doktora Tezi, University of Bern, İsviçre, 1999.
- 296 Thomas, J. N., Huard, J., Masci, F.: A statistical study of global ionospheric map total electron
297 content changes prior to occurrences of $M \geq 6.0$ earthquakes during 2000–
298 2014. *Journal of Geophysical Research: Space Physics*, 122(2), 2151-2161, 2017.
- 299 Yildirim, O., Inyurt, S., Mekik, C.: Review of variations in $M_w < 7$ earthquake motions on
300 position and TEC ($M_w = 6.5$ Aegean Sea earthquake sample). *Natural Hazards and*
301 *Earth System Sciences*, 16(2), 543-557, 2016.
- 302 URL-1 <https://omniweb.gsfc.nasa.gov/form/dx1.html>